KeAi
CHINESE ROOTS
GLOBAL IMPACT

Contents lists available at ScienceDirect

Defence Technology

journal homepage: www.keaipublishing.com/en/journals/defence-technology



Localization and tracking of multiple quadrotors with collision avoidance: Theory and experiment



Guang Yang ^a, Juntong Qi ^b, Mingming Wang ^{a, *}, Yan Peng ^b, Chong Wu ^c, Yuan Ping ^c, Hailong Huang ^d

- ^a The Tianjin Key Laboratory of Intelligent Unmanned Swarm Technology and System, School of Electrical and Information Engineering, Tianjin University, Tianjin, 300072, China
- ^b Institute of Artificial Intelligence, Shanghai University, Shanghai, 200444, China
- ^c EFY Intelligent Control (Tianjin) Technology Company Ltd., Tianjin, 300450, China
- ^d The Department of Aeronautical and Aviation Engineering, Hong Kong Polytechnic University, Hung Hom, Hong Kong, 999077, China

ARTICLE INFO

Article history: Received 11 January 2025 Received in revised form 25 February 2025 Accepted 2 April 2025 Available online 4 April 2025

Keywords: Multiple quadrotors Collision avoidance Target localization Tracking Outdoor experiments

ABSTRACT

Multiple quadrotors target encirclement is widely used in the intelligent field, as it can effectively monitor and control target behavior. However, it faces the danger of collision, as well as difficulties in localization and tracking. Therefore, we propose a complete target encirclement method. Firstly, based on Hooke's law, a collision avoidance controller is designed to maintain a safe flying distance among quadrotors. Then, based on the consensus theory, a formation tracking controller is designed to meet the requirements of formation transformation and encirclement tasks, and a stability proof based on Lyapunov was provided. Besides, the target detection is designed based on YOLOv5s, and the target location model is constructed based on the principle of pinhole projection and triangle similarity. Finally, we conducted experiments on the built platform, with 3 reconnaissance quadrotors detecting and localization 3 target vehicles and 7 hunter quadrotors tracking them. The results show that the minimum average error for localization targets with reconnaissance quadrotors can reach 0.1354 m, while the minimum average error for tracking with hunter quadrotors is only 0.2960 m. No quadrotors collision occurred in the whole formation transformation and tracking experiment. In addition, compared with the advanced methods, the proposed method has better performance.

© 2025 China Ordnance Society. Publishing services by Elsevier B.V. on behalf of KeAi Communications Co. Ltd. This is an open access article under the CC BY-NC-ND license (http://creativecommons.org/licenses/by-nc-nd/4.0/).

1. Introduction

Multiple quadrotors collaborative control technology has become a hot research topic in recent years [1–4]. It exhibits high efficiency, high fault tolerance, and good robustness when performing complex tasks, and has broad application prospects in military and civilian fields [5,6]. Target encirclement is one of the most common tasks, which enables real-time monitoring and control of target behavior [7,8]. For example, chasing target vehicles, escorting important targets, tracking suspicious targets, and so on [9,10].

However, the dense flight of multiple quadrotors brings the

possibility of collision, which leads to mission failure. On the other hand, the precise location of dynamic targets is difficult to obtain from the air, and how to establish a detection mechanism and localization model is a problem that needs to be solved urgently. At the same time, controlling multiple quadrotors to maintain stable encirclement and tracking of the target is also the key to success. Therefore, solving the problems of poor collision avoidance ability, difficult localization and tracking in multi-quadrotors target encirclement has become a challenge.

How to ensure the flight safety of multiple quadrotors is the primary issue in completing the encirclement. The artificial potential field method (APF) is a common collision avoidance method, which moves itself by repulsive force generated among quadrotors to achieve collision avoidance effect [11,12]. Yu et al. [13] introduced the APF method into the virtual leader formation scheme, utilizing local directional information exchange between quadrotors to ensure safe distance between them. Huang et al. [14] combined APF

^{*} Corresponding author.

E-mail address: wangmm19@tju.edu.cn (M. Wang).

Peer review under the responsibility of China Ordnance Society.

and particle swarm optimization techniques to provide environmental awareness and implicit coordination for quadrotors, searching for collision-free trajectories. Xia et al. [15] combined consensus control with APF method to achieve unmanned aerial vehicle (UAV) formation and dynamic collision avoidance. A simulation experiment was designed for a large UAV carrying some micro-UAVs, which verified the effectiveness of the proposed method. The APF method is simple in design, but it is easy to fall into the local optimal solution and jitter when approaching the collision. The idea of the method based on optimization is to solve the local path and realize the safe flight of the quadrotors without collision [16]. In Ref. [17], an improvement of the meta-heuristic African vulture optimization algorithm was proposed, which took collision avoidance as a constraint to obtain a smooth and collisionfree path. In Ref. [18], a geometric method for solving all collisionfree arrangements of UAVs had been proposed. On this basis, the performance index of the UAV was derived and optimized, and the optimal collision free arrangement in any direction was completed. The optimization-based method requires strong computing power and a long solving time, so it is not suitable for deployment on embedded platforms with low computing power. Therefore, a collision avoidance method with small computation and no local optimal restriction is needed. Hooke's law states that the elastic deformation of a spring under external force is proportional to the external force, and the damper can smoothly decelerate the controlled object [19]. In Ref. [20], a collision avoidance mechanism is designed using Hooke's law with damping, which overcomes the situation of falling into local optimal, and the potential field method is difficult to avoid the narrow passage in time.

In terms of multi-quadrotors formation tracking, the leaderfollower method is the most common [21]. Zhang et al. [22] used the leader guidance mechanism to establish the error dynamics model of each follower, and built the communication mode between any two UAVs based on graph theory to realize the regular triangle formation tracking task with the leader as the center and the follower as the vertex. Zhu et al. [23] designed coordinated control of multiple UAVs based on leader-follower method, and realized ring formation around the leading UAVs through simulation experiments, which verified the effectiveness of the proposed method. However, the leader-follower method relies too heavily on leader. The virtual structure method treats multiple UAVs as a whole and allows them to track the designed virtual target points to achieve formation flight. In Ref. [24], a method for controlling the transformation of quadrotors between different formations based on the virtual structure method was proposed. The virtual structure serves as a framework for planning the complex formation trajectories of multiple quadrotors. In Ref. [25], the quadrotor's kinematics was described as a multi-robot formation based on the virtual structure method, and the dynamic effects of the load are processed by an adaptive dynamic compensator. Two quadrotors were used to complete payload positioning, orientation, and trajectory tracking. But the virtual structure is highly dependent on a communication system with high robustness. The basic idea of the consensus theory is that each quadrotor carries out information interaction with its neighbor quadrotor and combines its state information to generate planning and control strategies, so that the whole multi-quadrotors system can achieve consistency in a certain state or behavior [26,27]. And consensus theory adopts distributed architecture, it has no nodes with global information. Distributed architecture has good scalability and fault tolerance. In Ref. [28], based on consensus theory, a control protocol was proposed and Lyapunov stability proofwas provided. A criterion in the form of linear matrix inequality was constructed to achieve the task of three quadrotors enclosing one quadrotor. In Ref. [29], the multiquadrotors formation algorithm based on consensus theory

ensures that the final convergence of each position was consistent, and the stability of the controller was proved using the Lyapunov function. In Ref. [30], a distributed dynamic event triggering mechanism based on consensus theory was designed to reduce communication burden and solve the problem of communication topology and formation structure changes caused by drone failures. This decentralized approach compensates for the shortcomings of the Leader follower. In Ref. [31], a position update algorithm was proposed based on consistency theory to address the collaborative search problem of unmanned aerial vehicles (UAVs) under unstable communication. This algorithm ensures that the position vectors of each UAV can reach consensus in a switched and connected topology, rejecting the leader of global information centralization.

The consensus theory has low requirements for real-time and connectivity of communication links and can be well applied to multi-quadrotors control system.

Some studies on multi-quadrotors encirclement and tracking do not have localization methods, but it is assumed that the position information of the target can be obtained within a certain range when the quadrotors approach the target [32,33]. With the increasing arithmetic power of embedded platforms, airborne computer vision can achieve an increasing number of tasks, and target localization through computer vision becomes possible. An increasing number of studies have attempted to combine computer vision and quadrotors to achieve more complex tasks [34,35]. In Ref. [36], a quadrotor recognition and localization quick-responsecodes were designed to achieve autonomous landing on unmanned vehicles, but the success rate of the experiment was not high. In Ref. [37], a relative localization system for micro aerial vehicles was developed, which can operate without any markings, but the localization error reaches the meter level. Therefore, how to accurately detect and locate the target has become an urgent problem to be solved.

Therefore, this paper proposes a complete multi-quadrotors encirclement framework that covers collision avoidance, formation tracking, and target localization. Among them, quadrotors are divided into reconnaissance quadrotors and hunting quadrotors. The reconnaissance quadrotors are responsible for detecting and locating targets, while the hunter quadrotors are responsible for encircling the targets. This paper conducted collision avoidance, localization, and tracking experiments using 3 reconnaissance quadrotors and 7 hunter quadrotors to verify the effectiveness of the proposed method. The main contributions can be summarized as the following four points:

- (1) Compared with the improved APF method [11,13–15], we propose a collision avoidance control method based on Hooke's law, and different repulsion functions are designed for quadrotors when approaching and moving away to ensure a safe distance between them. Meanwhile, it avoids getting stuck in local optima and jitter situations.
- (2) Compared with leader-follower method [21–23], we propose a tracking controller based on the consistency theory to drive multiple quadrotors to converge in position to meet the requirements of different formation tasks. Based on Lyapunov theory, it is proved that multiple quadrotors can track the dynamic target in formation. This decentralized distributed control method in this paper enhances the robustness of the system and reduces dependence on leaders.
- (3) Compared to the lack of object detection function in Refs. [32,33], propose a detection network based on YOLOv5s. And construct the target localization model based on pinhole projection and triangle similarity principle to complete the target localization. Compared to Refs. [36,37], reduced localization error.

(4) Built multiple quadrotors platforms, supporting 10quadrotors' experimental tasks such as formation transformation and encirclement. Compensated for the shortcomings of Refs. [15,23,29] that can only be verified through simulation experiments.

2. Problem description

Firstly, provide a model of the quadrotor. Define $\boldsymbol{p}_i = [p_{ix}, p_{iy}, p_{iz}]^{\mathrm{T}}$ and $\boldsymbol{v}_i = [\nu_{ix}, \nu_{iy}, \nu_{iz}]^{\mathrm{T}}$ as the position and velocity vectors of the quadrotor. Define $\boldsymbol{\Psi}_i = [\phi_i, \theta_i, \psi_i]^{\mathrm{T}}$ and $\boldsymbol{\Omega}_i = [g_i, q_i, r_i]^{\mathrm{T}}$ represent the Euler angles and angular rates of the quadrotor. The position subsystem and rotation subsystem are as follows:

$$\begin{cases} \dot{\boldsymbol{p}}_{i} = \boldsymbol{v}_{i} \\ m_{i}\dot{\boldsymbol{v}}_{i} = -m_{i}g\boldsymbol{e}_{3} + F_{i}R(\boldsymbol{\Psi}_{i})\boldsymbol{e}_{3} \\ \dot{\boldsymbol{\Psi}}_{i} = Y(\boldsymbol{\Psi}_{i})\boldsymbol{\Omega}_{i} \\ \boldsymbol{J}_{i}\dot{\boldsymbol{\Omega}}_{i} = -\boldsymbol{\Omega}_{i} \times \boldsymbol{J}_{i}\boldsymbol{\Omega}_{i} + \boldsymbol{\Gamma}_{i} \end{cases}$$

$$(1)$$

where g is gravitational acceleration F_i is the lifting force generated by the motors of the quadrotor. $J_i = \operatorname{diag}(J_{ix}, J_{iy}, J_{iz})$ is the moment of inertia, and $\Gamma_i \in \mathbb{R}^{3 \times 1}$ is the control torque. The orthogonal rotation matrix $R(\Psi_i)$ is shown below:

$$R(\boldsymbol{\Psi}_{i}) = \begin{bmatrix} C_{i}^{\theta}C_{i}^{\psi} & S_{i}^{\phi}S_{i}^{\theta}C_{i}^{\psi} - C_{i}^{\phi}S_{i}^{\psi} & S_{i}^{\phi}S_{i}^{\psi} + C_{i}^{\phi}S_{i}^{\theta}C_{i}^{\psi} \\ C_{i}^{\phi}S_{i}^{\psi} & S_{i}^{\phi}S_{i}^{\theta}S_{i}^{\psi} - C_{i}^{\phi}C_{i}^{\psi} & C_{i}^{\phi}S_{i}^{\theta}S_{i}^{\psi} - S_{i}^{\theta}C_{i}^{\psi} \\ -S_{i}^{\theta} & S_{i}^{\theta}C_{i}^{\theta} & C_{i}^{\phi}C_{i}^{\theta} \end{bmatrix}$$
(2)

The attitude kinematic matrix $Y(\Phi_i)$ is expressed as follows:

$$Y(\boldsymbol{\Psi}_{i}) = \begin{vmatrix} 1 & S_{i}^{\phi} T_{i}^{\theta} & C_{i}^{\phi} T_{i}^{\theta} \\ 0 & C_{i}^{\phi} & -S_{i}^{\phi} \\ 0 & S_{i}^{\phi} \left(C_{i}^{\phi} \right)^{-1} & C_{i}^{\phi} \left(C_{i}^{\theta} \right)^{-1} \end{vmatrix}$$
(3)

where *C*, *S*, and *T* are the abbreviations of $\cos(\cdot)$, $\sin(\cdot)$, and $\tan(\cdot)$, respectively.

The controller designed in this paper is for the translation subsystem of quadrotor. The translation subsystem can be written as follows:

$$\begin{cases}
\dot{p}_i(t) = v_i(t) \\
\dot{v}_i(t) = U_i^d(t)
\end{cases}$$
(4)

where the control signal $U_i^d(t) = F_i R(\Psi_i) e_3 / m_i - g e_3$. Next, design the controller for $U_i^d(t)$.

The control objective is to design collision avoidance and tracking controllers for the aforementioned quadrotor model to meet task requirements.

3. Main methodology

This section describes in detail the collision avoidance controller and tracking controller of multi-quadrotors, and provides proof of their stability. At the same time, the method of detecting and locating target by quadrotors is also introduced. Fig. 1 shows the schematic diagram of collision-free localization and tracking for

multiple quadrotors.

3.1. Collision avoidance

The primary requirement for multi-quadrotors formation flight is to ensure a safe distance among quadrotors, which requires the generation of repulsion when any two quadrotors approach, and the repulsion ensures smooth flight of the quadrotors. Therefore, this paper proposes a collision avoidance controller based on Hooke's law with damping. The controller designed in this paper has the following characteristics: (1) The effective area of the collision avoidance controller is clear: the collision avoidance controller plays a role when the distance between two quadrotors is less than R_c . At the same time, ensure that the distance between the two quadrotors is greater than the minimum safe distance R_s . (2) The collision avoidance controller presents different effects when the quadrotors are close to each other or away from each other: it generates greater repulsion when approaching to avoid collisions, and decreases repulsion when moving away to avoid colliding with other quadrotors. (3) The derivative of the collision avoidance function is continuous to obtain a smooth repulsion curve to ensure smooth flight of the quadrotors. Design the collision avoidance controller that meets the above requirements to achieve collision avoidance between multi-quadrotors. The following collision avoidance controller is designed for the

$$u_{i}^{c} = \begin{cases} \alpha \frac{1}{\left(\left\|\mathbf{p}_{ji} - R_{s}\right\|\right)^{2}} \frac{\mathbf{p}_{ji}}{\left\|\mathbf{p}_{ji}\right\|} + \beta v_{ji} & \left\|\mathbf{p}_{ji}\right\| \leq R_{c}, \mathbf{p}_{ji} \leq 0 \\ \alpha \frac{1}{\left(\left\|\mathbf{p}_{ji} - R_{s}\right\|\right)^{2}} \frac{\mathbf{p}_{ji}}{\left\|\mathbf{p}_{ji}\right\|} & \left\|\mathbf{p}_{ji}\right\| \leq R_{c}, \mathbf{p}_{ji} > 0 \\ 0 & \left\|\mathbf{p}_{ji}\right\| > R_{c} \end{cases}$$

$$(5)$$

where α and β are the positive gains. $\mathbf{p}_{ji} = \mathbf{p}_j - \mathbf{p}_i$ and $\mathbf{v}_{ji} = \mathbf{v}_j - \mathbf{v}_i$ are the position and velocity vectors between ith quadrotor and jth quadrotor, respectively.

Then, the convergence proof of the collision avoidance controller is given. Firstly, analyze the stability of case $\left\| \boldsymbol{p}_{ji} \right\| \leq R_c$, $\left\| \boldsymbol{p}_{ji} \right\| \leq 0$, and design a Lyapunov function as follows:

$$V_{ic1}(t) = \frac{1}{2} \sum_{j=1, j \neq i}^{N-1} \alpha \frac{1}{\|\mathbf{p}_{ji}\| - R_s} + \frac{1}{2} \sum_{j=1, j \neq i}^{N-1} \beta \int_0^t \mathbf{v}_{ji}^{\mathsf{T}}(\varsigma) \mathbf{v}_{ji}(\varsigma) d\varsigma$$
 (6)

Take the derivative of V_{ic1} .

$$V_{ic1}^{\cdot} = -\frac{1}{2} \sum_{j=1, j \neq i}^{N-1} \alpha \frac{1}{\left(\left\|\mathbf{p}_{ji} - R_{s}\right\|\right)^{2}} \left\|\mathbf{p}_{ji}\right\| + \frac{1}{2} \sum_{j=1, j \neq i}^{N-1} \beta \mathbf{v}_{ji}^{\mathsf{T}} \mathbf{v}_{ji}$$

$$= \sum_{j=1, j \neq i}^{N-1} \left[\alpha \frac{1}{\left(\left\|\mathbf{p}_{ji}\right\| - R_{s}\right)^{2}} \frac{\mathbf{p}_{ji}^{\mathsf{T}}}{\left\|\mathbf{p}_{ji}\right\|} - \beta v_{ji}^{\mathsf{T}} \right] \mathbf{v}_{i}$$
(7)

Consider the relationship between the velocity and the control input.

$$\mathbf{v}_i = \sum_{j=1, j \neq i}^{N-1} \mathbf{u}_{ij} \Delta t \tag{8}$$

Combining with Eqs. (5) and (8), it can be obtained that,

that the multi-quadrotors system is asymptotically convergent when $\|\mathbf{p}_{ii}\| \le R_c$, $\|\dot{\mathbf{p}}_{ii}\| > 0$. In summary, the stability proofof colli-

$$V_{ic1} = \left\{ \sum_{j=1, j \neq i}^{N-1} \left[\alpha \frac{1}{\left(\left\| \mathbf{p}_{ji} \right\| - R_{s} \right)^{2}} \frac{\mathbf{p}_{ji}}{\left\| \mathbf{p}_{ji} \right\|} - \beta \mathbf{v}_{ji} \right]^{T} \sum_{j=1, j \neq i}^{N-1} \left[-\alpha \frac{1}{\left(\left\| \mathbf{p}_{ji} \right\| - R_{s} \right)^{2}} \frac{\mathbf{p}_{ji}}{\left\| \mathbf{p}_{ji} \right\|} + \beta \mathbf{v}_{ji} \right] \right\} \Delta t$$

$$= \sum_{j=1, j \neq i}^{N-1} - \left[-\alpha \frac{1}{\left(\left\| \mathbf{p}_{ji} \right\| - R_{s} \right)^{2}} \frac{\mathbf{p}_{ji}}{\left\| \mathbf{p}_{ji} \right\|} + \beta \mathbf{v}_{ji} \right]^{T} \left[-\alpha \frac{1}{\left(\left\| \mathbf{p}_{ji} \right\| - R_{s} \right)^{2}} \frac{\mathbf{p}_{ji}}{\left\| \mathbf{p}_{ji} \right\|} + \beta \mathbf{v}_{ji} \right] \Delta t$$

$$(9)$$

According to Eq. (9), it can be obtained that $V_{ic1} \leq 0$. So multiquadrotor system is asymptotically convergent when $\| \boldsymbol{p}_{ji} \| \leq R_c$, $\| \boldsymbol{p}_{ji} \| \leq 0$.

Then, analyze the stability of case $\|\mathbf{p}_{ji}\| \le R_c$, $\|\mathbf{p}_{ji}\| > 0$. We design the following Lyapunov function.

$$V_{ic2} = \frac{1}{2} \sum_{j=1, j \neq i}^{N-1} \alpha \frac{1}{\|\mathbf{p}_{ji}\| - R_s}$$
 (10)

Calculate the derivative of V_{ic2}

$$\dot{V_{ic2}} = -\frac{1}{2} \sum_{j=1, j \neq i}^{N-1} \alpha \frac{1}{\left(\left\| \mathbf{p}_{ji} \right\| - R_{s} \right)^{2}} \left\| \dot{\mathbf{p}}_{ji} \right\|$$
(11)

Similarly, according to Eq. (11), we obtain $V_{ic2} \leq 0$. We also get

sion avoidance control has been completed.

Because of $V_{ic}(0) > 0$ and $\dot{V}_{ic}(t) \leq 0$, by combining Eqs. (6) and (10), we obtain $\frac{\alpha}{\|\boldsymbol{p}_{ji}\| - R_s} \leq V_i(0) < \infty$, and further obtain $\|\boldsymbol{p}_{ji}\| > R_s$. Therefore, under the action of the collision avoidance controller, there will be no collision among quadrotors.

3.2. Formation tracking control protocol

Multiple quadrotors should have the ability to fly in formation to complete tasks with different demands. This section proposes a quadrotors formation tracking controller based on consensus theory. First, algebraic graph theory is suitable for describing communication relationships between multiple quadrotors. The communication topology among quadrotors is depicted by a weighted directed graph $G = \{Q, E, W\}$: a node set Q, an edge set E and a weight set E. The degree matrix of the graph is defined as E0 = diagE1, where E2 is represents the number of edges entering the node E3, and the Laplacian matrix E5 of the graph is defined as E4 = E7 w.

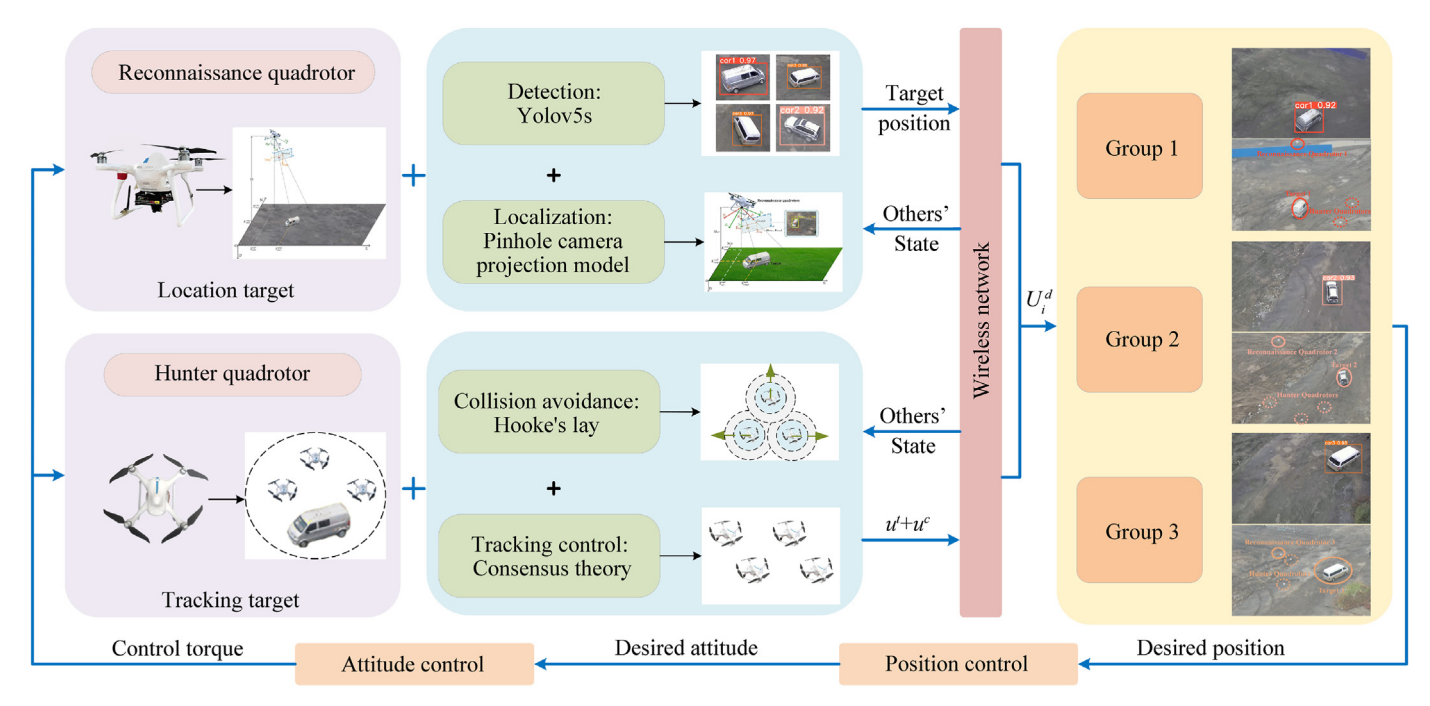


Fig. 1. Localization and tracking control scheme for multi-quadrotors with collision avoidance.

Lemma 1. Define $L \in \mathbb{R}^{N \times N}$ as the Laplacian matrix of the directed graph G. (1) L has a least one zero eigenvalue and $\mathbf{1}_N$ is the associated eigenvector. (2) If G has a spanning tree, then 0 is an eigenvalue of L, and all the other N-1 eigenvalues have positive real parts.

The tracking control law of the quadrotor is as follows:

$$u_i^t(t) = \mu \sum_{j=1}^N w_{ij} \left[(\vartheta_i(t) - \varrho_i(t)) - (\vartheta_j(t) - \varrho_j(t)) \right]$$

$$+ \mu (\vartheta_i(t) - \varrho_i(t) - \chi(t)) + \dot{\varrho}_{i\nu}(t)$$
(12)

where $\boldsymbol{\mu} \in \mathbb{R}^{1 \times 2}$ is constant gain matrix. $\vartheta(t) = \left[\boldsymbol{p}_i^T(t), \boldsymbol{v}_i^T(t)\right]^T (i=1,2,\cdots,N)$ represents the status of the quadrotor. $\varrho_i(t) = \left[\varrho_{ip}^T(t), \varrho_{iv}^T(t)\right]^T (i=1,2,\cdots,N)$ as the desired vector of the quadrotor formation. The state vector of the target is defined as $\chi(t) \in \mathbb{R}^{4 \times 1}$, and the detection and localization of the target is described in the next section.

Definition 1. A multi-quadrotor system under control protocol Eq. (12) can achieve target encirclement if $\lim_{t\to\infty} (\vartheta_i(t) - \varrho_i(t) - \chi(t)) = 0 (i = 1, 2, \dots N)$.

The system Eq. (4) can be rewritten as follows:

$$\dot{\vartheta}_i(t) = \mathbf{M}_1 \vartheta_i(t) + \mathbf{M}_2 u_i^t(t) \tag{13}$$

where $\mathbf{M}_1 = \begin{bmatrix} \mathbf{0}_2 & \mathbf{I}_2 \\ \mathbf{0}_2 & \mathbf{0}_2 \end{bmatrix}$, $\mathbf{M}_2 = \begin{bmatrix} \mathbf{0}_2 \\ \mathbf{I}_2 \end{bmatrix}$. Then, substituting Eq. (12) into Eq. (13).

$$\dot{\vartheta}(t) = \left[(\mathbf{I}_{N} \otimes \mathbf{M}_{1}) + \left(\mathbf{L}_{f} \otimes \mathbf{M}_{2} \boldsymbol{\mu} \right) \right]
\vartheta(t) - \left(\mathbf{L}_{f} \otimes \mathbf{M}_{2} \boldsymbol{\mu} \right) \varrho(t) + (\mathbf{I}_{N} \otimes \mathbf{M}_{2}) \dot{\varrho}_{\nu}(t) + (\mathbf{L}_{I} \otimes \mathbf{M}_{2} \boldsymbol{\mu}) \chi(t)$$
(14)

Define tracking error $\epsilon_i(t) = \vartheta_i(t) - \varrho_i(t)$. Using the Kronecker product, one obtains the following:

$$\dot{\epsilon}(t) = \left[(\mathbf{I}_{N} \otimes \mathbf{M}_{1}) + \left(\mathbf{L}_{f} \otimes \mathbf{M}_{2} \boldsymbol{\mu} \right) \right]
\epsilon(t) + (\mathbf{I}_{N} \otimes \mathbf{M}_{1}) \varrho(t) + (\mathbf{I}_{N} \otimes \mathbf{M}_{2}) \dot{\varrho_{\nu}}(t) - \dot{\varrho}(t)
+ (\mathbf{L}_{l} \otimes \mathbf{M}_{2} \boldsymbol{\mu}) \chi(t)$$
(15)

$$\dot{\varrho}(t) = (\mathbf{I}_N \otimes \boldsymbol{\xi})\dot{\varrho}_n(t) + (\mathbf{I}_N \otimes \mathbf{M}_2)\dot{\varrho}_n(t) \tag{16}$$

where $\boldsymbol{\xi} = \begin{bmatrix} \boldsymbol{I}_2 \\ \boldsymbol{0}_2 \end{bmatrix}$.

By substituting Eq. (16) into Eq. (15), we can obtain

$$\begin{split} \dot{\epsilon}(t) = & \left[(\mathbf{I}_{N} \otimes \mathbf{M}_{1}) + \left(\mathbf{L}_{f} \otimes \mathbf{M}_{2} \boldsymbol{\mu} \right) \right] \epsilon(t) + (\mathbf{I}_{N} \otimes \boldsymbol{\xi}) \left[\varrho_{v}(t) - \dot{\varrho}_{p}(t) \right] \\ & + (\mathbf{L}_{I} \otimes \mathbf{M}_{2} \boldsymbol{\mu}) \chi(t) \end{split}$$

Define $\overline{\epsilon}(t) = [\chi^{\mathrm{T}}(t), \epsilon^{\mathrm{T}}(t)]$, and take its derivative.

$$\dot{\overline{\backslash}} \epsilon(t) = \begin{bmatrix} \mathbb{MT} & \mathbf{0}_{4 \times 4N} \\ \mathbf{0}_{4N \times 4} & \mathbf{I}_N \otimes \mathbf{M}_1 \end{bmatrix} \overline{\epsilon}(t) + \begin{bmatrix} \mathbf{0}_{4 \times 4} & \mathbf{0}_{4 \times 4N} \\ \mathbf{L}_l \otimes \mathbf{M}_2 \mu & \mathbf{L}_f \otimes \mathbf{M}_2 \mu \end{bmatrix} \overline{\epsilon}(t) + \begin{bmatrix} \mathbf{0}_{4 \times 4N} \\ \mathbf{I}_N \otimes \boldsymbol{\xi} \end{bmatrix} [\varrho_{v}(t) - \dot{\varrho}_{p}(t)]$$
(18)

where \mathbb{MT} is the motion trajectory of the target, which is obtained by target localization.

Define a nonsingular matrix $\varpi = \begin{bmatrix} \mathbf{I}_N & \mathbf{1}_N \\ \mathbf{0}_{1\times N} & 1 \end{bmatrix}$. Combining $\mathbf{L}_l + \mathbf{L}_f \cdot \mathbf{1}_N = \mathbf{0}$, one obtains the following:

$$\begin{bmatrix} \mathbf{I}_{N} & -\mathbf{1}_{N} \\ \mathbf{0}_{1\times N} & 1 \end{bmatrix} \begin{bmatrix} \mathbf{L}_{f} & \mathbf{L}_{l} \\ \mathbf{0}_{1\times N} & 0 \end{bmatrix} \begin{bmatrix} \mathbf{I}_{N} & \mathbf{1}_{N} \\ \mathbf{0}_{1\times N} & 1 \end{bmatrix} = \begin{bmatrix} \mathbf{L}_{f} & \mathbf{0}_{1\times N} \\ \mathbf{0}_{1\times N} & 0 \end{bmatrix}$$
(19)

Define the target tracking error of quadrotors $e_t(t) = (\mathbf{I}_N \otimes \mathbf{I}_4) \epsilon(t) - (\mathbf{1}_N \otimes \mathbf{I}_4) \chi(t)$ and $\overline{e} = \left[\chi^{\mathrm{T}}(t), e_t^{\mathrm{T}}\right]^{\mathrm{T}}$. Then, one obtains that

$$\overline{e}(t) = \left(\varpi^{-1} \otimes \mathbf{I}_4\right)\overline{\epsilon}(t) \tag{20}$$

$$\overline{\epsilon}(t) = (\varpi \otimes \mathbf{I}_4)\overline{e}(t) \tag{21}$$

Pre-multiplying both sides of Eq. (18) by $\varpi^{-1} \otimes I_4$, one obtains that

$$\begin{split} &\dot{\overline{e}}(t) = \begin{bmatrix} \mathbb{MT} & \mathbf{0}_{4\times4N} \\ \mathbf{0}_{4N\times4} & \mathbf{I}_{N}\otimes\mathbf{M}_{1} \end{bmatrix} \overline{\mathbf{e}}(t) + \begin{bmatrix} \mathbf{0}_{4\times4} & \mathbf{0}_{4\times4N} \\ \mathbf{0}_{4N\times4} & \mathbf{L}_{f}\otimes\mathbf{M}_{2}\mu \end{bmatrix} \overline{\mathbf{e}}(t) \\ &+ \begin{bmatrix} \mathbf{0}_{4\times4N} \\ \mathbf{I}_{N}\otimes\boldsymbol{\xi} \end{bmatrix} \left[\varrho_{v}(t) - \dot{\varrho}_{p}(t) \right] \end{split} \tag{22}$$

Putting $\overline{e}(t) = \left[\boldsymbol{\chi}^{\mathrm{T}}(t), \boldsymbol{e}_{t}^{\mathrm{T}}(t) \right]^{\mathrm{T}}$ into Eq. (22).

$$\dot{e}_{t}(t) = \left[(\mathbf{I}_{N} \otimes \mathbf{M}_{1}) + \left(\mathbf{L}_{f} \otimes \mathbf{M}_{2} \boldsymbol{\mu} \right) \right] e_{t}(t) + (\mathbf{I}_{N} \otimes \boldsymbol{\xi}) \left(\varrho_{v}(t) - \dot{\varrho}_{p}(t) \right)$$
(23)

Theorem 1. For any given bounded initial state, the quadrotor can encircle the target if and only if $\lim_{t\to\infty} e_t(t) = 0$.

Proof: According to the Definition 1, a multi-quadrotor system under control protocol Eq. (12) can achieve target encirclement if $\lim_{t\to\infty} (\vartheta_i(t) - \varrho_i(t) - \chi(t)) = 0 (i=1,2,\cdots,N)$.

Due to
$$\epsilon_i(t) = \vartheta_i(t) - \xi_i(t)$$
 to $\theta_i(t) = \theta_i(t)$, then $\theta_i(t) = \theta_i(t)$ to $\theta_i(t) = \theta_i(t)$.

$$\lim_{t \to \infty} (\mathbf{I}_N \otimes \mathbf{I}_4) \epsilon(t) - (\mathbf{1}_N \otimes \mathbf{I}_4) \chi(t) = 0$$
 (24)

According to the definition of $e_t(t) = (\mathbf{I}_N \otimes \mathbf{I}_4)\epsilon(t) - (\mathbf{1}_N \otimes \mathbf{I}_4)\chi(t)$, that is, $\lim_{t \to \infty} e_t(t) = 0$. The proof of Theorem 1 ends.

Let $\lambda_i(\mathbf{L}_f)$ be the eigenvalue of \mathbf{L}_f , and $\phi \triangleq \min[\operatorname{Re}(\lambda_i(\mathbf{L}_f))]$, satisfying the following inequality.

$$\left(\mathbf{L}_{f}\right)^{\mathrm{T}}\mathbf{I}_{N}+\mathbf{I}_{N}\mathbf{L}_{f}-2\phi\mathbf{I}_{N}>0\tag{25}$$

Theorem 2. Under the tracking control law Eq. (12), the quadrotor can realize the desired formation if and only if: (i) $\lim_{t \to +\infty} [\varrho_{vi}(t) - \varrho_{vi}(t)] = \lim_{t \to +\infty} [\varrho_{vi}(t)] = \lim_{t \to +\infty}$

(17)

 $\dot{\varrho}_{pi}(t)]=0, \forall i=1,2,\cdots,N$, (ii) there exist a constant $\eta>0$ and a symmetric matrix P>0, which satisfies the following inequality: $M_1P+PM_1^T-M_2M_2^T+\eta P>0$.

Proof:

If condition (i) holds, one can be obtained that

$$\lim_{t \to +\infty} \left[\varrho_{\nu}(t) - \dot{\varrho}_{p}(t) \right] = 0 \tag{26}$$

Pre-multiply both sides of Eq. (26) by $I_N \otimes \xi$.

$$\lim_{t \to +\infty} (\mathbf{I}_N \otimes \xi) \left[\varrho_v(t) - \dot{\varrho}_p(t) \right] = 0 \tag{27}$$

So in Eq. (23), we only need to consider $[(I_N \otimes M_1) + (I_f \otimes M_2\mu)]\tilde{e}_t(t)$. Therefore, the definition of the replacement system is as follows:

$$\dot{\zeta}(t) = \left[\mathbf{I}_N \otimes \mathbf{M}_1 + \mathbf{L}_f \otimes \mathbf{M}_2 \boldsymbol{\mu} \right] \zeta(t) \tag{28}$$

Design the following Lyapunov function.

$$V_f(t) = \zeta^{\mathrm{T}}(t) \left(\mathbf{I}_N \otimes \mathbf{P}^{-1} \right) \zeta(t)$$
 (29)

Taking the derivative of it.

$$\dot{V}_{f}(t) = \zeta^{\mathrm{T}}(t) \left[\mathbf{I}_{N} \otimes \left(\mathbf{M}_{1}^{\mathrm{T}} \mathbf{P}^{-1} + \mathbf{P}^{-1} \mathbf{M}_{1} \right) + \mathbf{L}_{f}^{\mathrm{T}} \mathbf{I}_{N} \otimes (\mathbf{M}_{2} \boldsymbol{\mu})^{\mathrm{T}} \mathbf{P}^{-1} \right. \\
\left. + \mathbf{I}_{N} \mathbf{L}_{f} \otimes \mathbf{P}^{-1} \mathbf{M}_{2} \boldsymbol{\mu} \right] \zeta(t) \tag{30}$$

Let $\mu = -\tau M_2^{\rm T} P^{-1}$, and select a constant $\tau > 1/(2\phi)$. Then

$$\dot{V}_{f}(t) = \zeta^{T}(t) \left[\mathbf{I}_{N} \otimes \left(\mathbf{M}_{1}^{T} \mathbf{P}^{-1} + \mathbf{P}^{-1} \mathbf{M}_{1} \right) - \tau \left(\mathbf{L}_{f}^{T} \mathbf{I}_{N} + \mathbf{I}_{N} \mathbf{L}_{f} \right) \right]$$

$$\otimes \mathbf{P}^{-1} \mathbf{M}_{2} \mathbf{M}_{2}^{T} \mathbf{P}^{-1} \left[\zeta(t) \right]$$
(31)

Define $\zeta(t) = (\emph{\textbf{I}}_N \, \otimes \, \emph{\textbf{P}}) \kappa(t)$, one can obtain

$$\dot{V}_{f}(t) = \kappa^{\mathrm{T}}(t) \left[\mathbf{I}_{N} \otimes \left(\mathbf{P} \mathbf{M}_{1}^{\mathrm{T}} + \mathbf{M}_{1} \mathbf{P} \right) - \tau \left(\mathbf{L}_{f}^{\mathrm{T}} \mathbf{I}_{N} + \mathbf{I}_{N} \mathbf{L}_{f} \right) \otimes \mathbf{M}_{2} \mathbf{M}_{2}^{\mathrm{T}} \right] \kappa(t)$$
(32)

From Eq. (25) and Theorem 2, one can obtain

$$\dot{V}_f(t) \le \kappa^{\mathrm{T}}(t) \left[\mathbf{I}_N \otimes \left(\mathbf{M}_2 \mathbf{M}_2^{\mathrm{T}} - \eta \mathbf{P} \right) - 2\tau \phi \, \mathbf{I}_N \otimes \mathbf{M}_2 \mathbf{M}_2^{\mathrm{T}} \right] \kappa(t) \quad (33)$$

Since $\tau > 1/(2\phi)$ and $\kappa(t) = (\boldsymbol{I}_N \otimes \boldsymbol{P}^{-1})\zeta(t)$, one can obtain

$$\dot{V}_f(t) < \kappa^{\mathrm{T}}(t)(-\eta \mathbf{I}_N \otimes \mathbf{P})\kappa(t) = -\eta V_f(t) \tag{34}$$

Therefore, when conditions (i) and (ii) in Theorem 2 are met, the quadrotors can encircle and track the target with the desired formation. At this point, this proofis completed.

From Eqs. (5) and (12), the collision-free formation tracking controller for the quadrotor is designed as follows:

$$U_i^d(t) = \gamma_1 u_i^t(t) + \gamma_2 \sum_{j=1, j \neq i}^{N} u_{ij}^c(t)$$
(35)

where γ_1 and γ_2 are the gain coefficients of formation control and collision avoidance control, and the coefficients are adjusted according to different task requirements.

Finally, the parameters of rotation subsystem are calculated according to the control signals to achieve the desired flight control of the quadrotor. Recalling that $U_i^d(t) = -ge_3 + \tilde{F}_i/m_i$, the attitude

angle can be calculated as follows:

$$\begin{cases} \theta_{i} = \arctan \frac{U_{ix}^{d} C_{i}^{\psi} + U_{iy}^{d} S_{i}^{\psi}}{U_{iz}^{d} + g} \\ \phi_{i} = \arcsin \frac{U_{ix}^{d} S_{i}^{\psi} - U_{iy}^{d} C_{i}^{\psi}}{\sqrt{\left(U_{ix}^{d}\right)^{2} + \left(U_{iy}^{d}\right)^{2} + \left(U_{iz}^{d} + g\right)^{2}}} \\ \psi_{i} = \psi_{i}^{0} \end{cases}$$
(36)

where ψ_i^0 is the initial yaw angle of the quadrotor.

The roll and pitch are not restricted, and the yaw is restricted to a fixed angle to ensure that the quadrotor does not rotate.

3.3. Target detection and localization

The reconnaissance quadrotor is responsible for target detection and localization. Firstly, design a target detection module based on YOLOv5s. The collected RGB images are resized and padded to $416 \times 416 \times 3$ for preprocessing. The backbone network adopts CSPDarknet for feature extraction, which maintains efficiency while improving the accuracy and speed of the model. The neck fusion backbone network extracts different levels of features using feature pyramid network (FPN) and path aggregation network (PAN) structures. FPN downsamples the rich semantic features downstream, while PAN upsamples the more precise localization information contained in the underlying layers upstream. The prediction performs post-processing on the output of the network, and finally obtains the target vehicle's category, confidence level, and pixel coordinates of the target center through non-maximum suppression (NMS). Finally, the pixel coordinates of the target center are input into the target localization module.

Target localization is the process of converting the center pixel coordinates of the target vehicle into 3D North East Down (NED) coordinates. Firstly, based on the pinhole camera projection model [38], convert the pixel coordinates ($u_{\rm target}$, $v_{\rm target}$) into positions in the image coordinate system.

$$P^{\text{img}} = \left(\frac{u_{\text{target}} - c_x}{dx}, \frac{v_{\text{target}} - c_y}{dy}, f\right)$$
(37)

Due to the need for quadrotors to locate ground target vehicles from the air, the reconnaissance quadrotor is equipped with a camera between -45° pitch angle. we denote the pitch, yaw, roll of quadrotor, and camera tilt as P, Y, R, and T, respectively. The attitude of the camera changes with the attitude of the quadrotor. The camera's rotation $R_{\rm cam}$ is:

$$\mathbf{R}_{cam} = \begin{bmatrix} C_{Y}C_{R} & -C_{Y}S_{R}C_{T} + S_{Y}S_{T} & C_{Y}S_{R}S_{T} + S_{Y}C_{T} \\ S_{R} & C_{R}C_{T} & -C_{R}S_{T} \\ -S_{Y}C_{R} & S_{R}S_{Y}C_{T} + C_{Y}S_{T} & -S_{R}S_{Y}S_{T} + C_{Y}C_{T} \end{bmatrix}$$
(38)

By combining Eq. (38), we can obtain the target position in the camera coordinates of the quadrotor.

$$\begin{bmatrix} x_{\text{target}}^{qc} \\ y_{\text{target}}^{qc} \\ f^{qc} \end{bmatrix} = \mathbf{R}_{\text{cam}} \begin{bmatrix} \frac{u_{\text{target}} - c_x}{dx} \\ \frac{v_{\text{target}} - c_y}{dy} \\ f \end{bmatrix}$$
(39)

Next, based on the principle of triangle similarity, the height of the quadrotor is used as the depth source to recover the threedimensional position of the target.

$$\begin{cases} X_{\text{target}}^{c} = \frac{(H_{\text{qua}} - \iota_{\text{ht}} \cdot H_{\text{target}}) x_{\text{target}}^{qc}}{y_{\text{target}}^{qc}} \\ Y_{\text{target}}^{c} = H_{\text{qua}} - \iota_{\text{ht}} \cdot H_{\text{target}} \\ Z_{\text{target}}^{c} == \frac{(H_{\text{qua}} - \iota_{\text{ht}} \cdot H_{\text{target}}) f^{qc}}{y_{\text{target}}^{qc}} \end{cases}$$

$$(40)$$

where H_{qua} is the height of quadrotor. ι_{ht} is the parameter for the target height, with a value of 0.5, to obtain the center height of the target vehicle.

Due to the camera being installed in the center position below the quadrotor, translation errors are ignored. Finally, obtain the coordinates of the target vehicle in the NED coordinate system:

$$\begin{cases} X_{\text{target}}^{\text{ned}} = X_{\text{qua}}^{\text{ned}} + Z_{\text{target}}^{c} \\ Y_{\text{target}}^{\text{ned}} = Y_{\text{qua}}^{\text{ned}} + X_{\text{target}}^{c} \\ Z_{\text{target}}^{\text{ned}} = \iota_{\text{ht}} \cdot H_{\text{target}} \end{cases}$$
(41)

where $X_{\text{qua}}^{\text{ned}}$ and $Y_{\text{qua}}^{\text{ned}}$ are the NED coordinates of the quadrotor. At this point, the target vehicle status $\gamma(t)$ is obtained.

4. Experimental results

This section first introduces the constructed quadrotor platform, and then verifies the effectiveness of the proposed method through several outdoor experiments. It is recommended to watch the video to understand the experimental scene and results better. It can be found at: https://www.bilibili.com/video/BV1KWhoekEvR.

4.1. Multiple quadrotors platform

This paper builds a multiple quadrotors platform as shown in Fig. 2, which mainly consists of multiple quadrotors, WiFi, real-time kinematic (RTK), base station, and ground station. The parameters of quadrotors are shown in Table 1. The quadrotor is mainly equipped with RTK positioning module, communication module. single board computer (SBC) and flight controller system (FCS). The RTK module is responsible for receiving positioning data and completing real-time positioning of the quadrotors. The communication module provides communication functions with other quadrotors and ground stations. SBC is responsible for running the onboard control program and transmitting the resolved control commands to the flight controller through a serial port. The main function of the FCS is to measure and control the attitude and position of a quadrotors. Besides, the reconnaissance quadrotor added a monocular camera and a Jetson Xavier NX onboard computer to detect and locate the unmarked moving target vehicle. The ground station is mainly responsible for monitoring the status of quadrotors and issuing control commands, such as locking, landing, or returning, and does not participate in the control of quadrotors. The relevant parameters of these modules are shown in Table 2. The algorithm runs at a frequency of 20 Hz during the experiment, while the angular rate control of the quadrotor runs at a frequency of 250 Hz.

The experimental platform (Including all reconnaissance quadrotors and hunter quadrotors) constructs a communication link based on Message Queuing Telemetry Transport (MQTT) protocol. MQTT protocol specifies two types of network entities: message brokers and clients. The message broker acts as a server, receiving messages from the client and sending them to the target client. Then, the clients get the messages by subscribing to the specified Topic. MQTT protocol has lower memory and CPU overhead compared to the Robot Operating System (ROS), and it is a lightweight communication protocol based on publish/subscribe

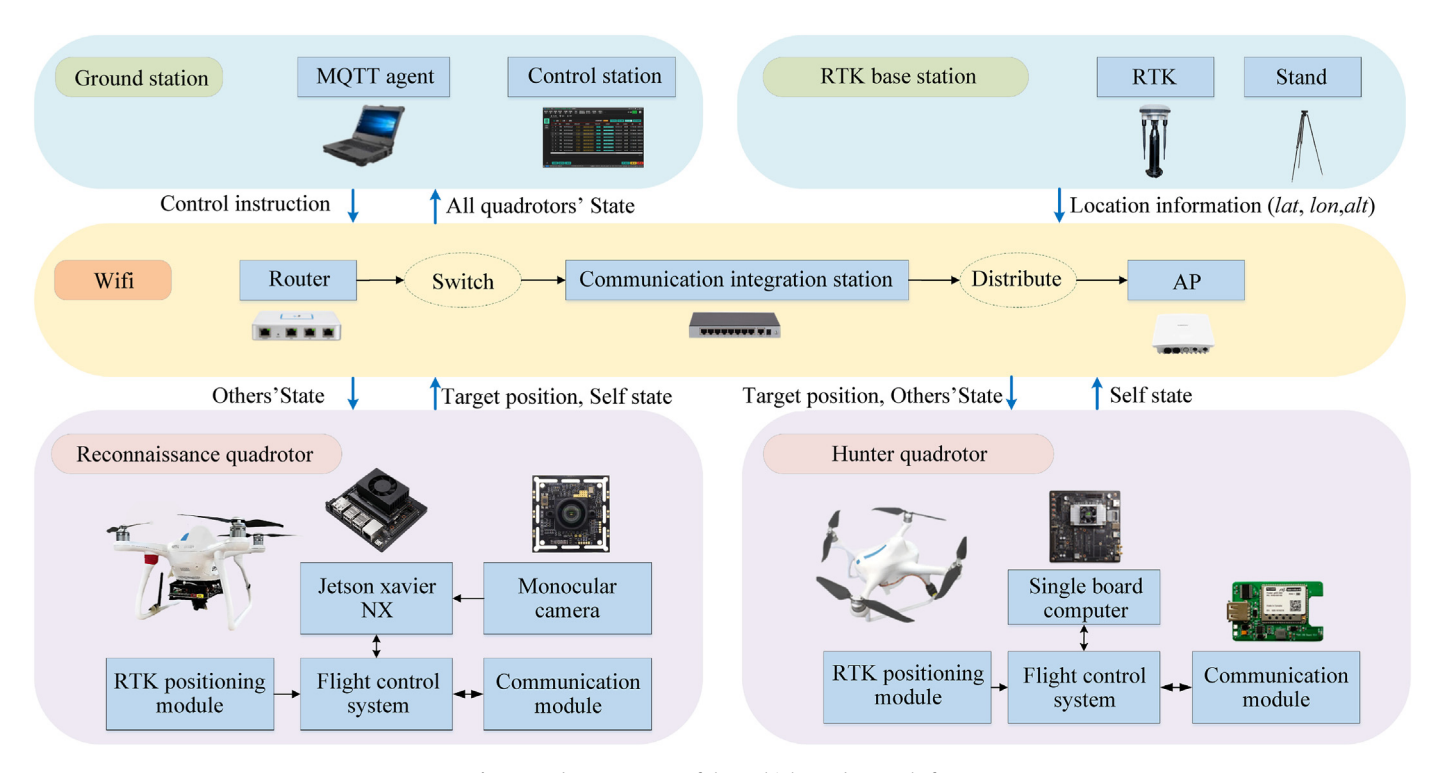


Fig. 2. Hardware structure of the multiple quadrotors platform.

Table 1The relevant parameters of quadrotor.

Parameters	Diagonal wheelbase	Weight	Battery life	Maximum load	Maximum flying speed
Numerical values	350 mm	1460 g	30 min	500 g	10 m·s ⁻¹

Table 2The relevant parameters of modules.

Modules	Specification	Key parameters and part numbers
RTK positioning module	U-blox ZED-F9P	Resolution ±2 cm (RTK), update frequency 1 Hz
communication module	RTL8812CU	Frequency band: 2.4/5 GHz, transmission range: 200 m
SBC	i.MX 6ULL	CPU: Cortex-A7, working frequency: 792 MHz
FCS	Pixhawk2.4.8	CPU: STM32F427 CortexM4, working frequency: 168 MHz

paradigm, which is suitable for communication between devices with poor hardware performance. In this paper, the message agent runs on the ground station computer, and the quadrotor serves as the client. At the physical layer, message brokers and clients transmit messages through a Wireless Local Area Network (WLAN) with a frequency band of 2.4 GHz and a bandwidth of 20 MHz–40 MHz. The communication frequency is 20 Hz, and the communication information mainly includes position information (longitude, latitude, altitude) and velocity information (north direction, east direction, ground direction). The type of information is floating-point, double precision, and 64 Bit.

4.2. Collision avoidance experiment

It should be noted that the collision avoidance controller plays a role throughout the entire flight mission. In the formation transformation experiment here, multiple quadrotors cross fly and change positions according to requirements, which better reflects the role of the collision avoidance controller. The parameter of

collision avoidance is selected as $R_c = 2.2$ m, $R_s = 1.3$ m, $\alpha = 10$ and $\beta = 2$. To ensure flight safety, we set the maximum flight velocity of quadrotors to 1.2 m/s during the collision avoidance phase.

Fig. 3(a) shows collision avoidance trajectories of multiple quadrotors, with different colors representing different quadrotor's groups. The starting point of seven hunter quadrotors are (-28, 28), (-28, 36), (-24, 28), (-24, 36), (-20, 28), (-20, 6), (-20, 44), with a formation of three lines. The quadrotors finally reach three circles with (-37, 42), (-40, 30) and (-45, 13) as the center and a radius of 5 m. 7 hunter quadrotors changed from line to three circles. Fig. 3(b) shows the experimental phenomena at different times, the quadrotors almost completed its formation transformation at t = 39 s. A safe distance is maintained between the quadrotors and no collisions occurred. Besides, the flight trajectory of the quadrotor is smooth. And as can be seen from Fig. 4, the velocity of all quadrotors drops to zero after the formation transformation is completed, verifying the effectiveness of the proposed collision avoidance controller.

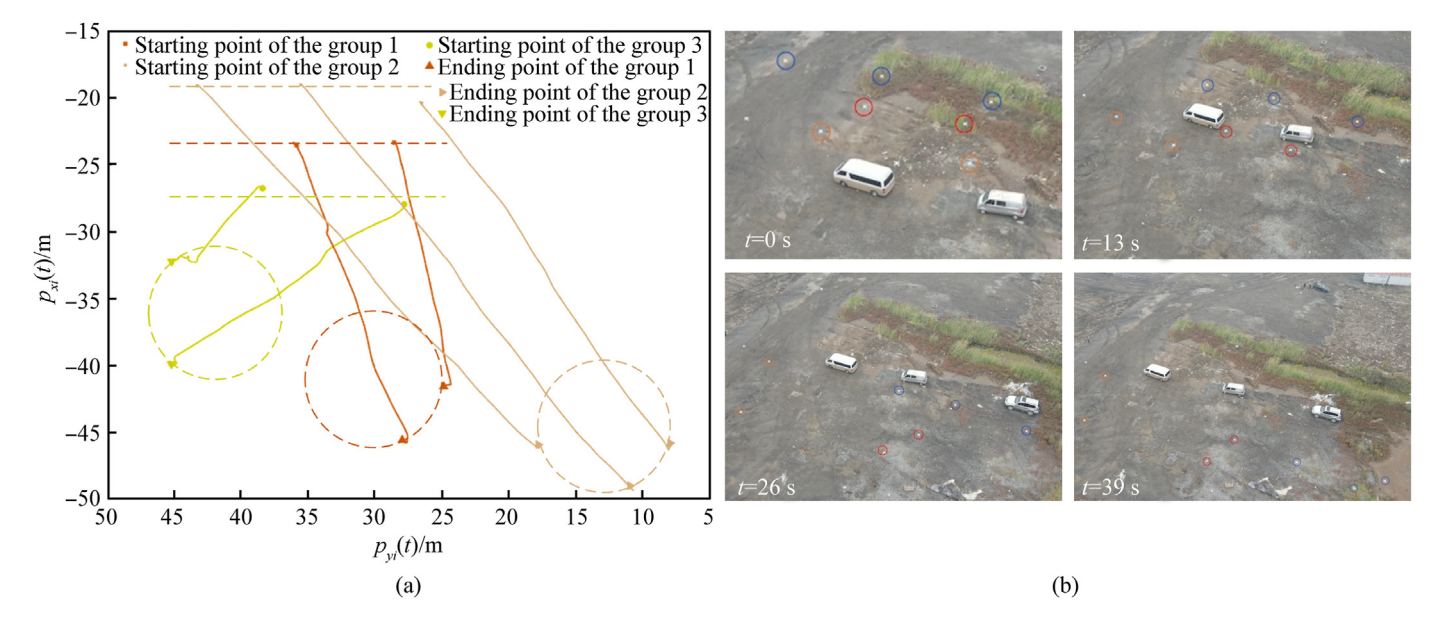


Fig. 3. Collision avoidance experiment situation: (a) Flight trajectory; (b) Four moments of aerial view.

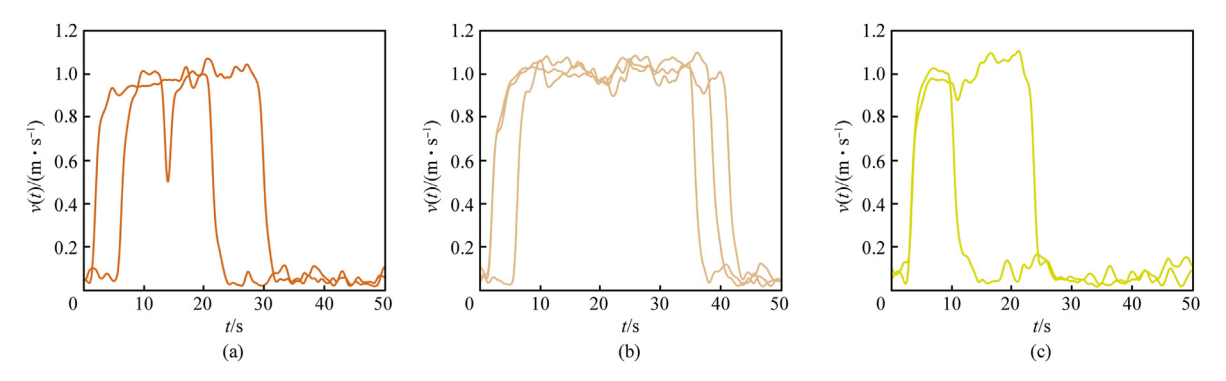


Fig. 4. Three groups of quadrotors velocity in collision avoidance experiments: (a) The first group; (b) The second group; (c) The third group.



Fig. 5. Target detection at four moments in the localization and tracking experiment.

4.3. Target localization and tracking experiment

In this experiment, 3 reconnaissance quadrotors detect and locate their target vehicles at heights of 14 m, 16 m, and 5 m, respectively, and send real-time localization results to each group of hunter quadrotors to complete the encirclement of the target vehicles. In order to keep up with the target movement, the

maximum flight velocity of quadrotors is no longer limited during the tracking phase.

Fig. 5 shows the object detection situation at four time points, and the recognition confidence reaches a high level. Fig. 6(a) shows the trajectory of the quadrotors tracking the target vehicle, where the trajectories of 3 vehicles are represented by dashed lines, and the trajectories of each group of quadrotors are represented by solid

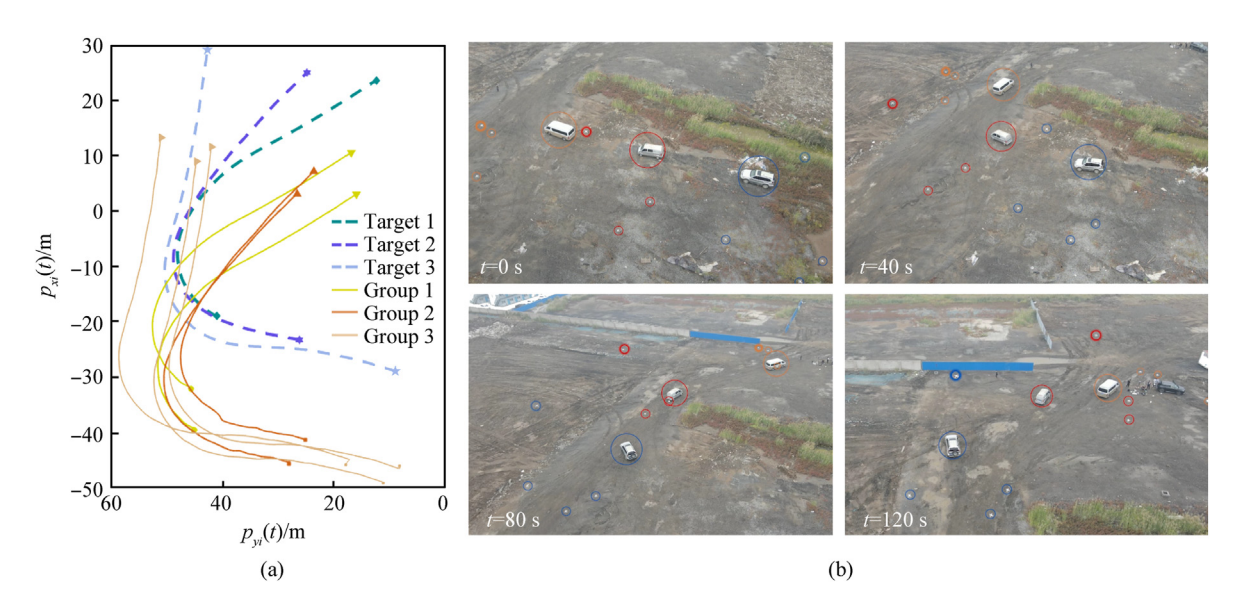


Fig. 6. Localization and tracking experimental process and trajectory: (a) Flight trajectory; (b) Four moments of aerial view.

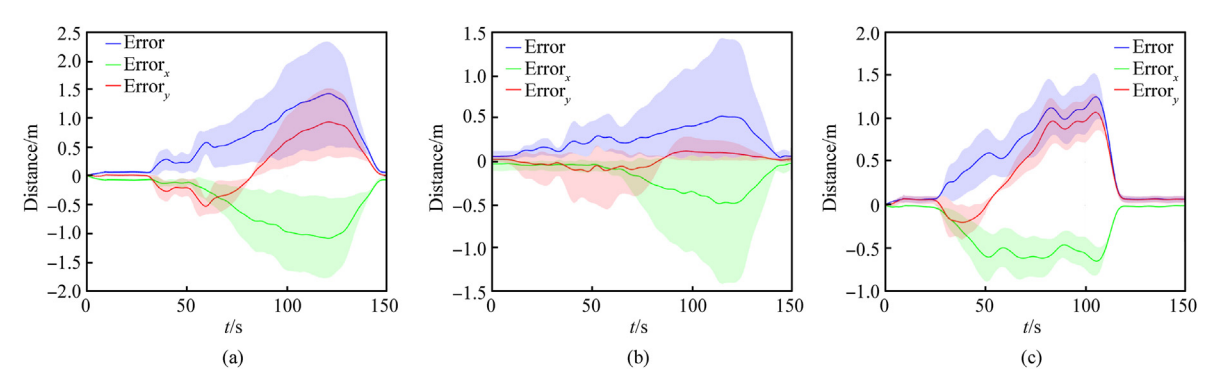


Fig. 7. Hunter quadrotors tracking error profiles: (a) The first group; (b) The second group; (c) The third group.

Table 3 Experimental situation.

Group	Tracking error (Max)/m	Tracking error (Ave)/m	Localization error (Max)/m	Localization error (Ave)/m
No.1	2.3373	0.7652	1.6781	0.5199
No.2	1.4323	0.2960	1.3677	0.1354
No.3	1.5277	0.7445	1.1987	0.4873

lines of different colors. We can see that each quadrotor moves accordingly to the trajectory of the target vehicle. It should be noted that we installed GPS on the target vehicle to compare the localization and tracking errors of the algorithm. At the same time, to ensure the safety of vehicles and people, each group of quadrotors tracks behind the target vehicle. Fig. 6(b) shows four moments when three groups of quadrotors track the target vehicle, during which the quadrotors closely follow the vehicle. 10 quadrotors each performed their respective duties and successfully completed the mission requirements.

Figs. 7(a)—(c) show in detail the tracking errors of three groups of quadrotors. The blue, green, and red lines represent errors the total, *X*-axis, and *Y*-axis directions, respectively. It can be seen that each group of quadrotors maintains a small range of errors. Table 3 uses quantitative data to measure tracking and localization effectiveness. The maximum localization error is 1.6781 m and the good locating ability of reconnaissance quadrotors to target vehicle provides the basis for the tracking of hunter quadrotors. The maximum average tracking error of the three groups of quadrotors is 0.7652 m. The above results validate the effectiveness of the proposed localization and tracking method.

Fig. 8 shows the roll and pitch angle of the quadrotor in outdoor experiments, and the yaw angle remains unchanged, so it is not shown. It can be seen that there is no sudden change in roll and pitch angle throughout the entire experimental phase, which ensures the smooth flight of the quadrotors. Meanwhile, the roll and pitch angle are calculated according to Eq. (36), which also proves the effectiveness of the proposed method.

4.4. Algorithm comparison

In order to verify the progressiveness of the proposed method, it is compared with APF and leader-follower methods in collision avoidance and formation tracking. We design the same experiment that 5 quadrotors encircle and track 1 quadrotor, and the results are shown in Fig. 9. Each method displays the flight trajectory, velocity,

tracking error, and distance between adjacent quadrotors separately.

Compared to the APF and the leader-follower method, the method proposed in this paper has a smoother flight, and the encirclement formation is also maintained the best. The velocity oscillation is the smallest, and it can be seen from Table 4 that the encircled formation is formed in the shortest time. Compared with APF and leader-follower, the time efficiency is improved by 4.04% and 32.32%, respectively. Similarly, our proposed approach minimizes the average tracking error of quadrotors, which is only 0.0764 m. Besides, the safest distance between the quadrotors is maintained throughout the flight and tracking process. This paper uses the nonparametric Wilcoxon signed-rank test to investigate the differences between the three methods. The significance level is set at 0.05. Another five groups of control experiments are added, and the target's movement trajectory is different. The proposed method can encircle the target more quickly (APF: $p = 3.03 \times 10^{-2}$, Leader-follower: $p = 4.30 \times 10^{-3}$). The tracking error is also smaller than the other two methods (APF: $p = 2.60 \times 10^{-2}$, Leader-follower: $p = 8.70 \times 10^{-3}$). We use the computation time to measure the complexity of the algorithm. The relevant parameters of the computer are shown in Table 5. It can be seen from the computation time that the computational complexity of the proposed method is lower (APF: $p = 8.70 \times 10^{-3}$, Leader-follower: $p = 2.60 \times 10^{-2}$). This proves that the computational complexity of the proposed method is low, and it does not need to rely on strong hardware performance. From the results, it can be seen that the proposed method has better performance.

5. Conclusions

In this work, a localization and tracking method for multiple quadrotors with collision avoidance is proposed. Based on that, 3 reconnaissance quadrotors detect and locate targets, and 7 hunter quadrotors encircle them. Deploy the algorithm on the developed multi-quadrotors platform to verify the effectiveness of the

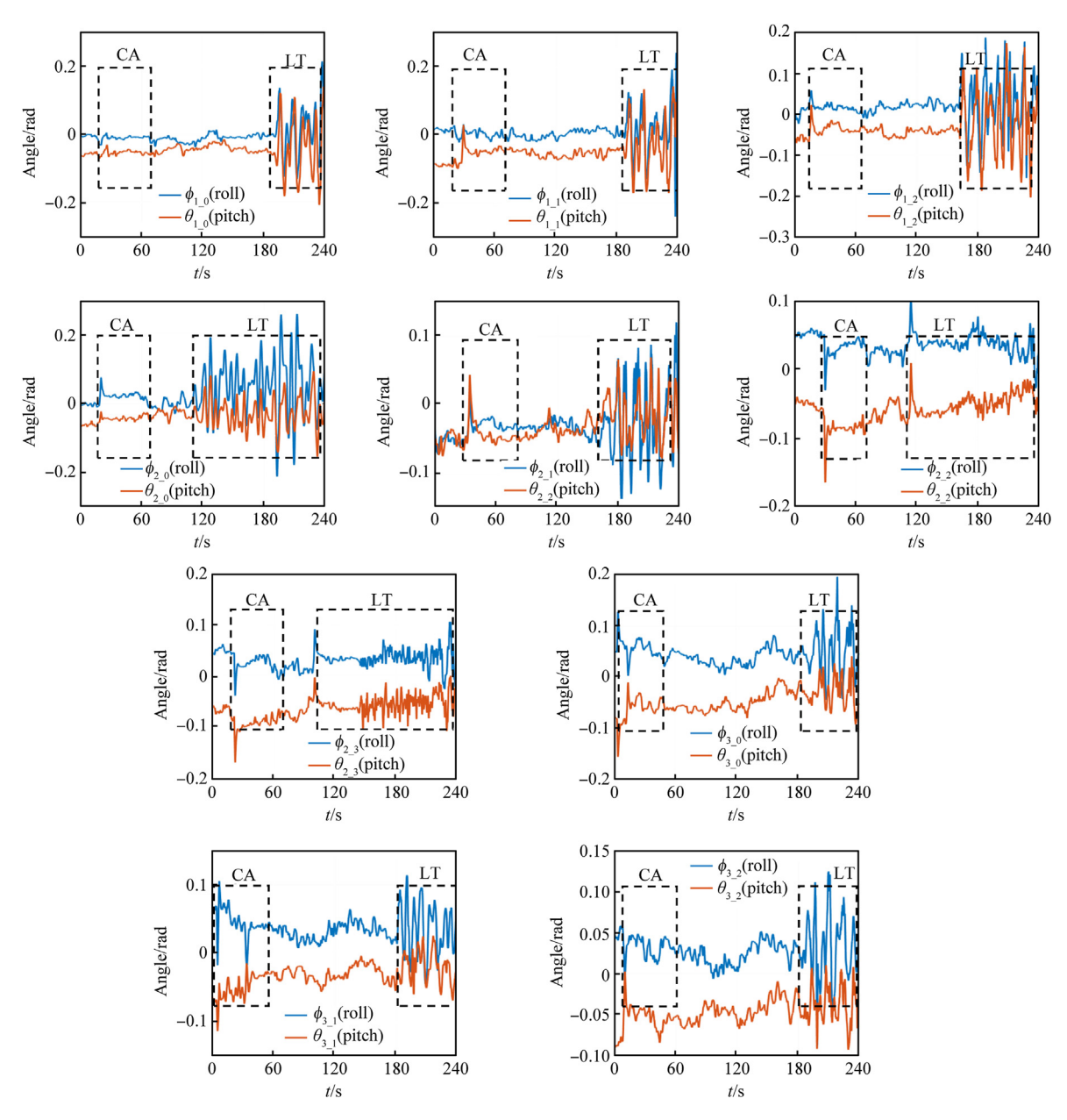


Fig. 8. Angle of quadrotors in collision avoidance (CA) and tracking (LT) experiments.

method. The results show that quadrotors can successfully avoid collisions, while localization and tracking targets with small errors. The proposed method is superior to the advanced comparison method in the performance of encirclement completion time, tracking error and safety distance between quadrotors. This provides suggestions for multiple quadrotors to encircle targets. In the future work, we will increase the obstacle avoidance function and enhance the theoretical contribution. In addition, platform validation for more than 10 quadrotors missions will be conducted to

enhance technical capabilities.

CRediT authorship contribution statement

Guang Yang: Writing — review & editing, Writing — original draft, Visualization, Validation, Methodology, Investigation, Formal analysis, Data curation, Conceptualization. **Juntong Qi:** Resources, Project administration, Funding acquisition. **Mingming Wang:** Supervision, Funding acquisition. **Yan Peng:** Supervision,

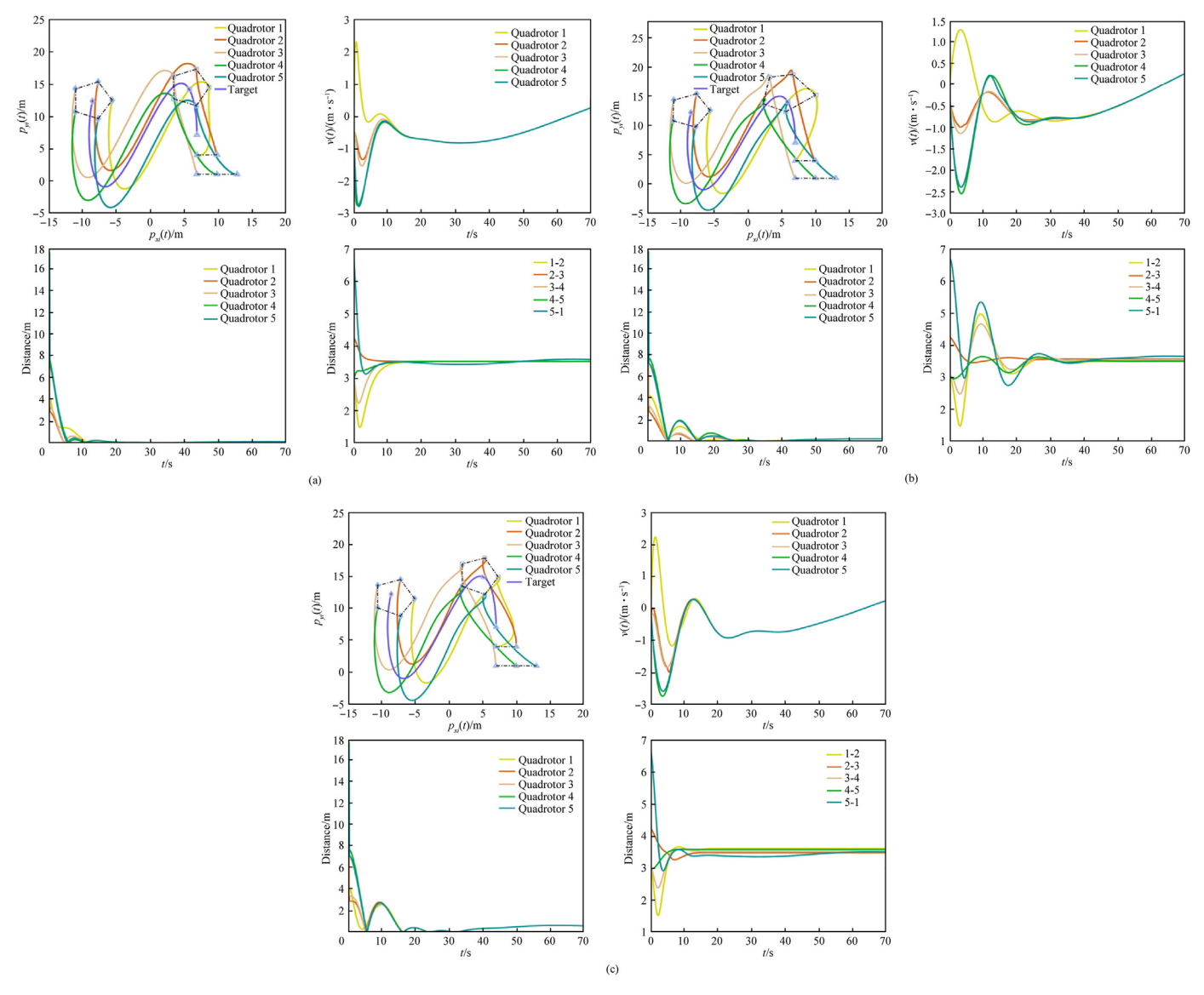


Fig. 9. Performance comparison results of three methods: (a) Proposed method; (b) APF method; (c) Leader-follower method.

Table 4 Method performance comparison.

Method	Encirclement completion time	Distance between quadrotors (Min)	Tracking error (Max)	Computation time
The proposed approach	9.9 s	1.3325 m	0.3254 m	3.2000 ms
APF	10.3 s	1.0289 m	1.9145 m	3.3585 ms
Leader-follower	13.1 s	0.7926 m	1.5551 m	3.3657 ms

Table 5The relevant parameters of computer.

Modules	Specification	Key parameters and part numbers
CPU	i7-13700H	Maximum frequency 5 GHz, a total of 14 cores, 20 threads
GPU	GeForce RTX 3090	24 GB memory capacity, 1400 MHz core frequency
Hard disk	Intel S4520	Read speed: 550 MB/s, Write speed: 510 MB/s

Resources. **Chong Wu:** Supervision, Project administration. **Yuan Ping:** Supervision, Project administration. **Hailong Huang:** Supervision, Resources.

Declaration of competing interest

The authors declare that they have no known competing financial interests or personal relationships that could have appeared to influence the work reported in this paper.

Acknowledgements

The authors would like to acknowledge the National Natural Science Foundation of China (Grant Nos. 62303348 and 62173242), the Aeronautical Science Foundation of China (Grant No. 2024M071048002), and the National Science Fund for Distinguished Young Scholars (Grant No. 62225308) to provide fund for conducting experiments.

References

- [1] Zheng D, Zhang YF, Li F. UAVs cooperative task assignment and trajectory optimization with safety and time constraints. Def Technol 2023;20(2): 149–61.
- [2] Yang P, Zhang A, Bi W. Cooperative group formation control for multiple quadrotors system with finite-and fixed-time convergence. ISA Trans 2023;138:186–96.
- [3] Park BS, Yoo SJ. Time-Varying formation control with moving obstacle avoidance for input-saturated quadrotors with external disturbances. IEEE T Syst Man Cy B 2024;54(5):3270–82.
- [4] Ai X, Yu J. Flatness-based finite-time leader—follower formation control of multiple quadrotors with external disturbances. Aero Sci Technol 2019;92: 20–33
- [5] Yuksel T. Fuzzy gain-scheduling based fault to lerant visual servo control of quadrotors, Drones 2023;7(2):100.
- [6] Hage C, Sophy T, Aglzim EH. Investigating UAV propellers performances near moving obstacles: CFD study, thrust control, and battery energy management. IEEE Open J Vehicular Technol 2023;4:590–609.
- [7] Hafez AT, Marasco AJ, Givigi SN. Solving multi-UAV dynamic encirclement via model predictive control. IEEE Trans Control Syst Technol 2015;23(6): 2251–65.
- [8] Shao X, Yue X, Zhang W. Coordinated moving-target encircling control for networked quadrotors with event-triggered extended state observers. IEEE Syst J 2023;17(4):6576–87.
- [9] Shao X, Yue X, Zhang W. Target encircling control possessing decreased sampling load for quadrotors with experimental verification. Mechatronics 2023;96:103090.
- [10] Song G, Xu J, Deng L. Robust distributed fixed-time cooperative hunting control for multi-quadrotor with obstacles avoidance. ISA Trans 2024;151: 73–85.
- [11] Yan X, Jiang D, Miao R, et al. Formation control and obstacle avoidance algorithm of a multi-USV system based on virtual structure and artificial potential field. J Mar Sci Eng 2021;9(2):161.
- [12] Yang Y, Shu Z, Liu Q. Predictor-based collision-free and connectivity-preserving resilient formation control for multi-agent systems under sensor deception attacks. Int J Robust Nonlin 2024;34(12):7968–91.
- [13] Yu Y, Chen C, Guo J. Adaptive formation control for unmanned aerial vehicles with collision avoidance and switching communication network. IEEE Trans Fuzzy Syst 2024;32(3):1435–45.
- [14] Huang S, Zhang H, Huang Z. E^ 2CoPre: energy efficient and cooperative collision avoidance for UAV swarms with trajectory prediction. IEEE T Intell

- Transp 2024;25(7):6951-63.
- [15] Xia Q, Zhou X, Song D. Cooperative formation control method for unmanned aerial vehicle cluster based on less sensor data. Sensor Mater 2023;35.
- [16] Yu Q, Luo L, Liu B. Re-planning of quadrotors under disturbance based on meta reinforcement learning. J Intell Rob Syst 2023;107(1):13.
- [17] Ait-Saadi A, Meraihi Y, Soukane A. An enhanced African vulture optimization algorithm for solving the unmanned aerial vehicles path planning problem. Comput Electr Eng 2023;110:108802.
- [18] Jamshidifar H, Khajepour A. Static workspace optimization of aerial cable towed robots with land-fixed winches. IEEE Trans Robot 2020;36(5): 1603–10.
- [19] Guo J, Qi J, Wang M. Distributed cooperative obstacle avoidance and formation reconfiguration for multiple quadrotors: theory and experiment. Aero Sci Technol 2023:136:108218.
- [20] Guo J, Qi J, Wang M. Collision-free distributed control for multiple quadrotors in cluttered environments with static and dynamic obstacles. IEEE Rob Autom Lett 2023;8(3):1501–8.
- [21] Yang H, Cheng L, Zhang J. Leader-follower trajectory control for quadrotors via tracking differentiators and disturbance observers. IEEE T Syst Man Cy A 2018;51(1):601–9.
- [22] Zhang J, Yan J, Zhang P. Multi-UAV formation control based on a novel back-stepping approach. IEEE Trans Veh Technol 2020;69(3):2437–48.
- [23] Zhu S, Wang D, Low CB. Cooperative control of multiple UAVs for moving source seeking. In: International conference on unmanned aircraft systems (ICUAS); 2013. p. 193–202. Atlanta, USA.
- [24] Zhou D, Wang Z, Schwager M. Agile coordination and assistive collision avoidance for quadrotor swarms using virtual structures. IEEE Trans Robot 2018;34(4):916–23.
- [25] Villa DKD, Brandão AS, Carelli R. Cooperative load transportation with two quadrotors using adaptive control. IEEE Access 2021;9:129148–60.
- [26] Dong X, Yu B, Shi Z. Time-varying formation control for unmanned aerial vehicles: theories and applications. IEEE Trans Control Syst Technol 2014;23(1):340–8.
- [27] Huang M, Lu Q. A fixed-time hierarchical formation control strategy for multiquadrotors. J Robot 2021;2021.
- [28] Wang M, Sun L, Ping Y. Formation encirclement of multiple quadrotors subjected to semi-Markov jump switching topologies under consensus strategy. Int J Robust Nonlin 2023;33(12):6932–49.
- [29] Chen X, Fan Y, Wang G. Coordinated control of quadrotor suspension systems based on consistency theory. Aerospace 2023;10(11):913.
- [30] Wei L, Chen M, Shi S. Dynamic event-triggered consensus cost-based switching control for UAV formation with disturbances. IEEE Transaction on Intelligent Vehicles 2024;9(2):3531–43.
- [31] Zhang H, Ma H, Mersha BW. Distributed cooperative search method for multi-UAV with unstable communications. Appl Soft Comput 2023;148.
- [32] Guo J, Qi J, Wang M. Collision-free formation tracking control for multiple quadrotors under switching directed topologies: theory and experiment. Aero Sci Technol 2022;131:108007.
- [33] Dong X, Zhou Y, Ren Z, et al. Time-varying formation tracking for secondorder multi-agent systems subjected to switching topologies with application to quadrotor formation flying. IEEE Trans Ind Electron 2016;64(6): 5014–24.
- [34] Zhou H, Lynch J, Zekkos D. Autonomous wireless sensor deployment with unmanned aerial vehicles for structural health monitoring applications. Struct Control Hlth 2022;29(6):e2942.
- [35] Outay F, Mengash HA, Adnan M. Applications of unmanned aerial vehicle (UAV) in road safety, traffic and highway infrastructure management: recent advances and challenges. Transport Res A-Pol 2020;141:116–29.
- [36] Niu G, Yang Q, Gao Y. Vision-based autonomous landing for unmanned aerial and ground vehicles cooperative systems. IEEE Rob Autom Lett 2021;7(3): 6234–41.
- [37] Vrba M, Saska M. Marker-less micro aerial vehicle detection and localization using convolutional neural networks. IEEE Rob Autom Lett 2020;5(2):
- [38] Wang W, Xie E, Song X. Efficient and accurate arbitrary-shaped text detection with pixel aggregation network. In: Proceedings of the IEEE/CVF international conference on computer vision; 2019. p. 8440–9. Seoul, South Korea.